ISSN (Print) 1226-1750
ISSN (Online) 2233-6656
Journal of Magnetics 27(2), 147-154 (2022) https://doi.org/10.4283/JMAG.2022.27.2.147

Comparison of Electromagnetic Performance according to Winding Configuration for Modular Dual 3-Phase Permanent Magnet Machines

Jangho Seo*

School of Automotive Engineering, Kyungpook National University, Sangju 37224, Republic of Korea

(Received 21 June 2021, Received in final form 5 April 2022, Accepted 5 April 2022)

A new winding structure for modular dual 3-phase permanent magnet machine, which makes it possible to reduce mutual coupling between two-winding sets of inverters and interference between phases that belong to the same inverter has been proposed in this study. The modular dual 3-phase system with overlapping winding technique has been widely employed in large-scale machine applications such as wind power production; however, its drawbacks include large torque ripple, long end-winding, and large magnetic mutual interference. To address these problems, a new modular dual 3-phase winding can be achieved by replacing adjacent redundant coils in one of the same phase coils with nonoverlapping winding. For clarity, three dual 3-phase machines are selected to examine their differences. The first is 32-poles/96-slots adopting a conventional overlapping modular winding ('Conv-1'), the second is 32-poles/36-slots based on the conventional nonoverlapping winding ('Conv-2'), and the other is 32-poles/36-slots adopting the proposed modular winding configuration ('Proposed'). The validity of the proposed structure is confirmed from simulation results obtained using finite element analysis.

Keywords : Dual 3-phase, permanent magnet, wind power generation, winding

1. Introduction

Recently, dual 3-phase machines have been widely studied because of advancements in power converter technology and increased demand for system reliability [1]. This machine incorporates identical winding; each independently supplied by a separate converter whose Volt-Amps rating corresponds to half-machine power (Fig. 1). This technique has the benefit of not requiring custom converters, which are necessary for five-phase or other multi-phase machines [1].

Over the past few decades, the dual 3-phase machines that adopt integer slot overlapping (OL) winding have gained much attention [2-7]. However, induction machines have attracted the most interest. Models of any displaced angle between two sets of windings have been reported [6]. Luigi Alberti showed the impact of winding arrangement on machine performance including fault tolerance [7]. However, the performance of machines with OL winding exhibit a large torque ripple, and the mutual magnetic coupling remains unsolved.

Since the introduction of nonoverlapping (NOL) fractional slot windings in permanent magnet (PM) machines [8-15], research for dual 3-phase machines with NOL winding has significantly increased [11-15]. In [11], the torque performance of 10-poles/12slots PM machines with dual 3-phase was investigated under good and faulty conditions. The mutual coupling between the winding sets was also identified [13, 14]. Xu *et al.* proposed a specific 15° angle displacement between two winding sets, different from the conventional zero and thirty angles, and exhibited better performance, particularly under short-circuit conditions [15].

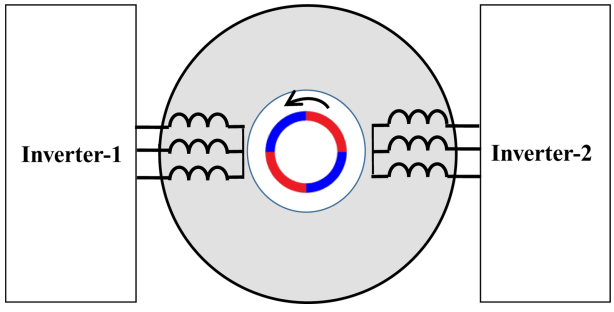

Fig. 1. (Color online) Scheme of a dual 3-phase motor drive.

©The Korean Magnetics Society. All rights reserved.
*Corresponding author: Tel: +82-54-530-1408
Fax: +82-54-530-1409, e-mail: j.seo@knu.ac.kr

© 2022 Journal of Magnetics

Modularity in large-scaled electrical machine design, such as wind power generators, is mandatory because the core of large-sized electrical machines cannot be manufactured.

Though a conventional two-layer NOL winding can be modularized, exposing the sides of the coil at the end of each segment to air increases the risk of coil damage. Further, large mutual flux exists between adjacent coils of single-layer NOL windings [8, 9], which make them unsuitable for dual 3-phase systems. Some studies satisfy both magnetic fields decoupling between winding sets and modular stator structure concurrently.

To resolve the above-mentioned problems, a new winding structure for modular dual 3-phase PM machines is proposed by removing adjacent redundant coil in one of the same phase coils with NOL winding. Three machines have been designed to compare machine performances. The first of the machines has 32-poles/96-slots with a conventional modular OL winding ('Conv-1'), the second has 32-poles/36-slots with a conventional NOL winding ('Conv-2'), and the other has 32-poles/36-slots with a proposed modular NOL winding ('Proposed'). The importance of the proposed winding will be established by comparing the 2-D finite element analysis results of back-electromotive force (back-EMF), torque ripple, losses, and inductances.

2. Proposed Winding Configuration

Figure 2 depicts an example of winding connections of OL and NOL winding. Notably, only “A” phase coils are expressed, and their magnetomotive force (MMF) waveforms are shown in Fig. 3. It is easily observed that no mutual flux by zero MMF zone exists in the NOL winding using two adjacent coils, but a clear mutual flux exists between the coils in the OL winding.

Figure 4 shows the conceptional transformation from 2-layer NOL winding to the proposed modular winding structure. The transformation rules are as follows.

1) A suitable pole-slot combination that satisfies the three adjacent coils is selected. In Fig. 4, 32-poles 36-slots is chosen, following the equation [14]:

$$3 = \frac{Q}{m\left|Q - 2p\right|} \tag{1}$$

where '3' means the number of coils placed in succession, m is the phase number, Q is the slot number and p is the pole pair.

2) A coil at the end of the three adjacent coils is removed. Then, the residual two coils can have the same conditions as Fig. 2(b).

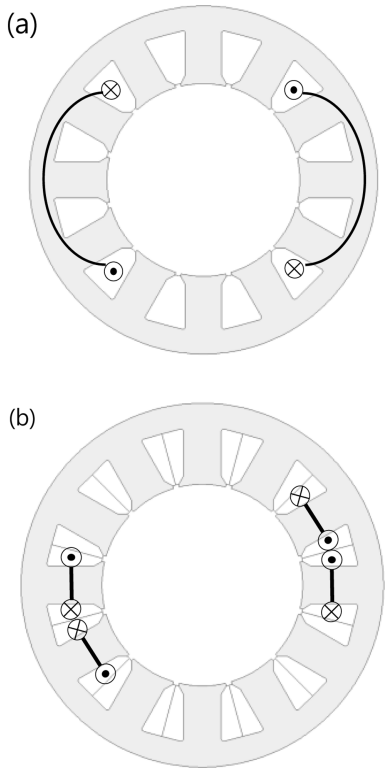

Fig. 2. Winding connection of A-phase coil. (a) 4-poles 12-slots motor having OL winding. (b) 10-poles 12-slots motor with NOL winding.

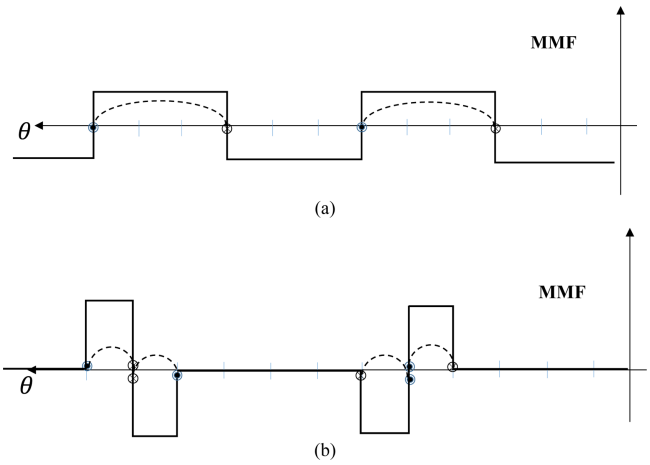

Fig. 3. (Color online) Armature MMF distribution. (a) 4 poles/12 slots motor (with M ≠ 0). (b) 10 poles/12 slots motor (with M = 0).

3) The coil span is adjusted to get a large winding factor. Careful adjustment is required because the coil span can induce large cogging torque. Fig. 5 illustrates back-EMF according to the coil span adjustment. The amplitude of the back-EMF increases with the coil span to a certain point, which implies the existence of magnetic

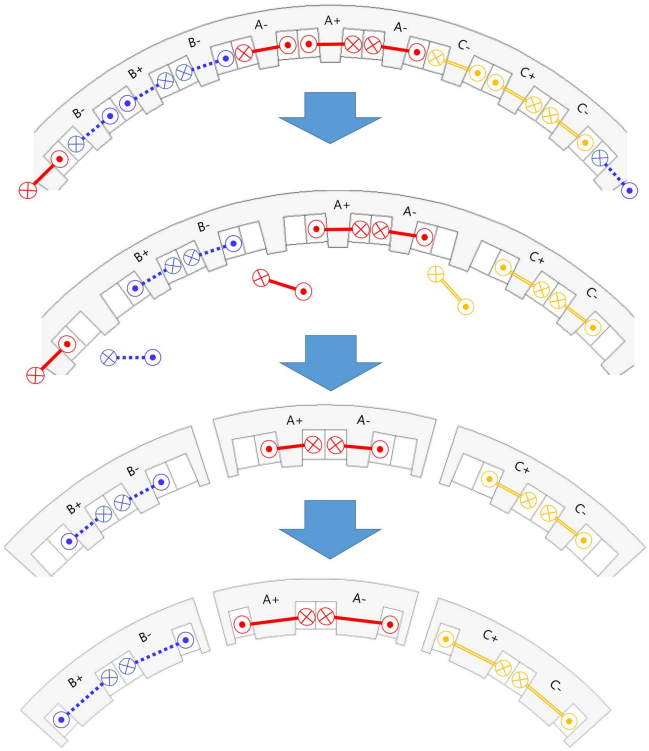

Fig. 4. (Color online) The conceptual transformation from a conventional 2-layer winding to a proposed modular winding.

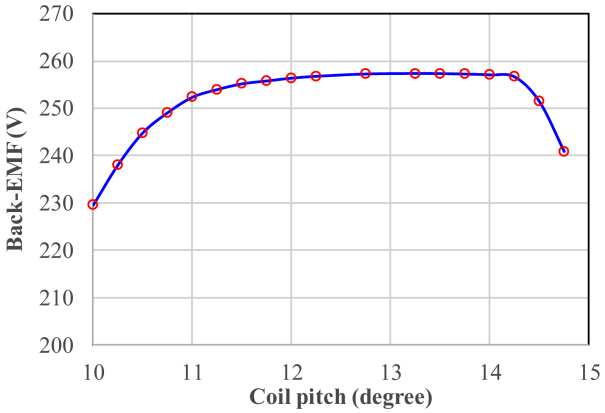

Fig. 5. (Color online) Back-EMF of a proposed winding with different coil pitch widths.

saturation between the segment stator core.

From Fig. 5, the coil pitch is selected as 13.5°. Cross-sectional views of the two modular machines are shown in Fig. 6. The 'Conv-1' with conventional modular winding consists of 16 segments, whereas the machine adopting the proposed winding configuration ('Proposed') consists of 12 segments. A1, B1, and C1 mean 3-phase A, B, C coils connected to inverter-1, and A2, B2, and C2 means A, B, C coils connected to inverter-2.

To maintain equal armature excitation, the rated current

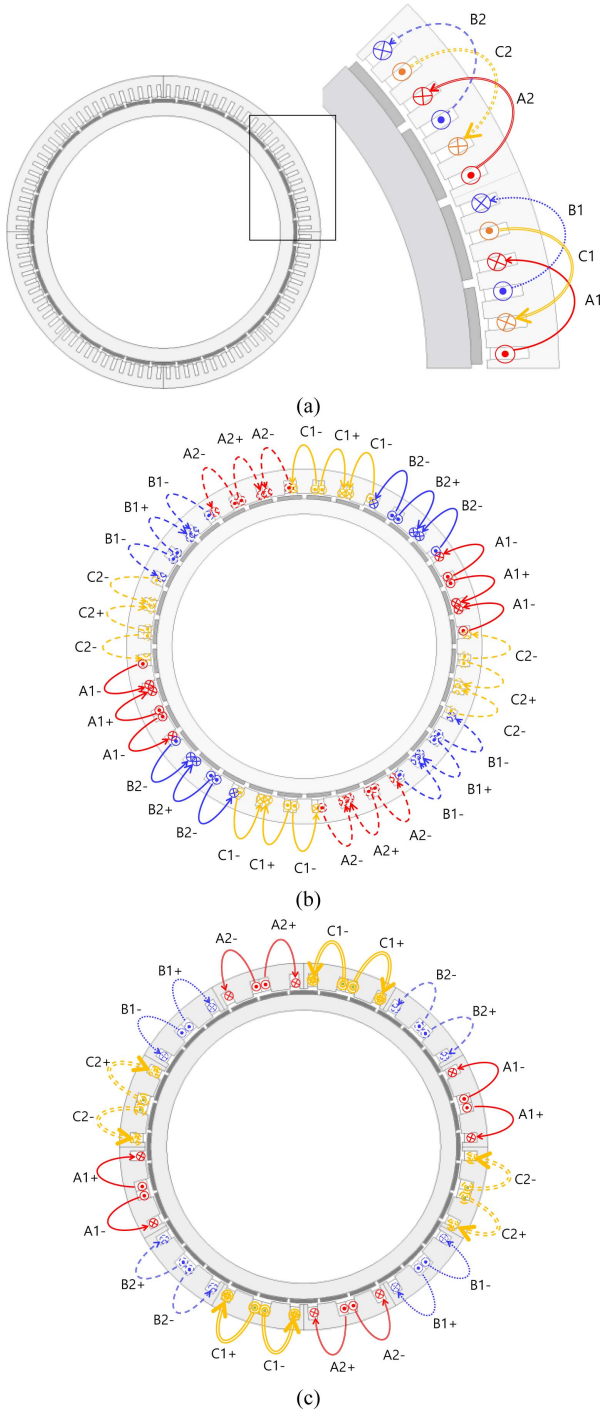

Fig. 6. (Color online) Cross-section of two motors. (a) Conv-1. (b) Conv-2. (c) Proposed.

and turns per phase are kept constant. Their specification is listed in Table 1.

3. Performance Comparison

Figure 7 shows the field distribution under open-circuit

Table 1. Design parameters and dimensions of the analysis model.

Parameters	Conv-1	Conv-2	Proposed
Pole	32	32	32
Slot number	96	36	36
Modular	yes	no	yes
Winding type	OL	NOL	NOL
Turns per phase		432	
Stator outer diameter (mm)		430	
Stator inner diameter (mm)		370	
Air gap length (mm)		2	
Axial length (mm)		110	
PM remanence (B_r)		1.2	
Rated speed (rpm)		170	
Rated current (Arms)		3.1	
Ratio of pole arc to pole pitch ratio		0.9	
Slot fill factor (%)		50.0	
Current density [Arms/mm^2]		3.6	

conditions. Whereas Conv-1 and Conv-2 has evenly distributed flux density level, the Proposed is more saturated toward the end of the segment because the coil span is increased, as illustrated in Fig. 5.

Figure 8(a) shows the flux density waveforms in the machines' air gaps under open-circuit condition and their harmonic orders are shown in Fig. 8(b). Within 50 orders, the Conv-1 has just two harmonic components, i.e., the rotor pole pair number (16th) and 48th, whereas the Conv-2 and Proposed have two subharmonic orders. Since the Conv-2 and Proposed have a larger slot opening length compared with the Conv-1, its effective air gap length will be larger and the corresponding working harmonic magnitude become lower than that of Conv-1.

Figure 9 shows the estimated back-EMFs under a rated speed of 170 r/min. Since the phase shift angle between A1 and A2 is zero, the identical waveforms can be confirmed. In addition, Fig. 9 shows that the Conv-1 with conventional modular winding type exhibits a more

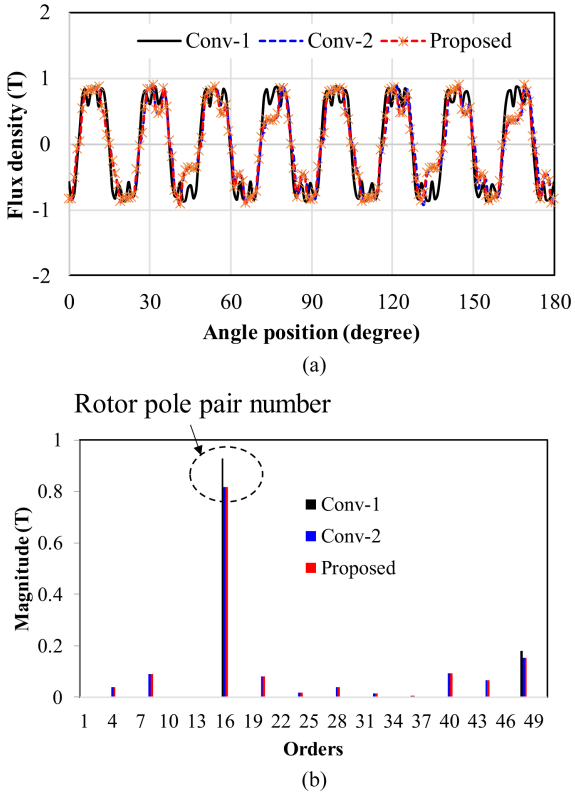

Fig. 8. (Color online) Air gap flux density under open-circuit PM field distribution. (a) Waveforms. (b) Harmonic orders.

trapezoidal back-EMF compared to the others. However, it has the largest fundamental amplitude of back-EMF thanks to its large air-gap flux density as shown in Fig. 8.

Figure 10 presents the comparison of the cogging torque waveforms. The Conv-1 with OL winding has a much larger cogging torque than the others. The Conv-2 and Proposed has a smaller cogging toque because the least common multiple in its number of poles and slots is 288, which is significantly larger than that of Conv-1 having 96.

Figure 11 shows the torque ripple waveforms generated

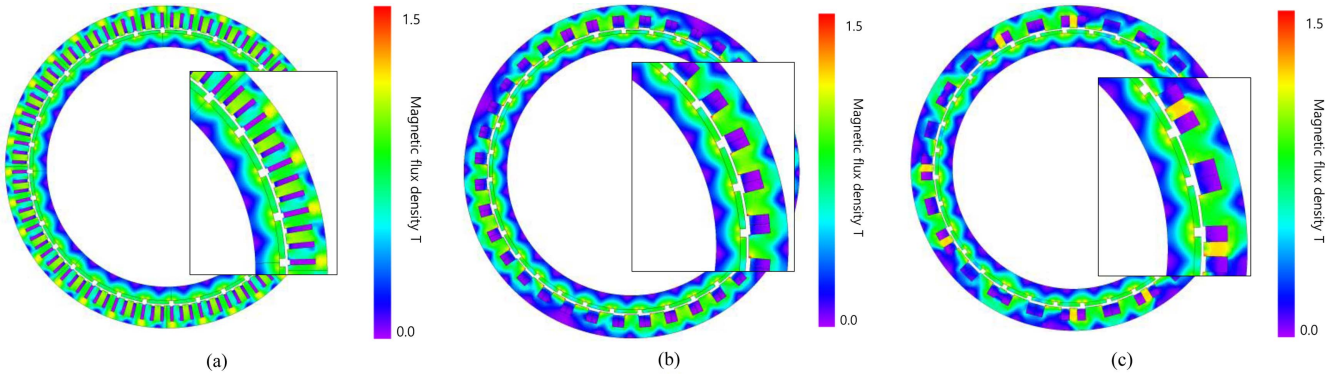

Fig. 7. (Color online) Open-circuit PM field distribution. (a) Conv-1. (b) Conv-2. (c) Proposed.

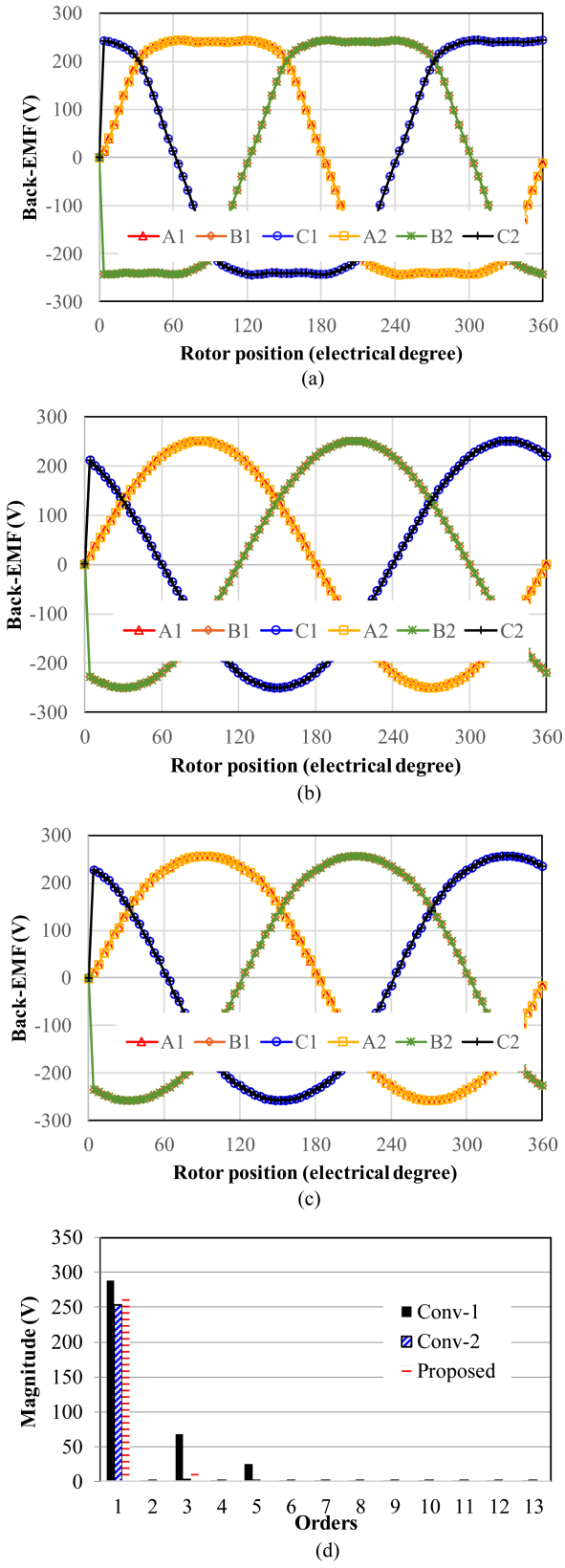

Fig. 9. (Color online) Phase back-EMFs under open-circuit (170 r/min). (a) Conv-1. (b) Conv-2. (c) Proposed. (d) Harmonic orders of A1 back-EMF waveform.

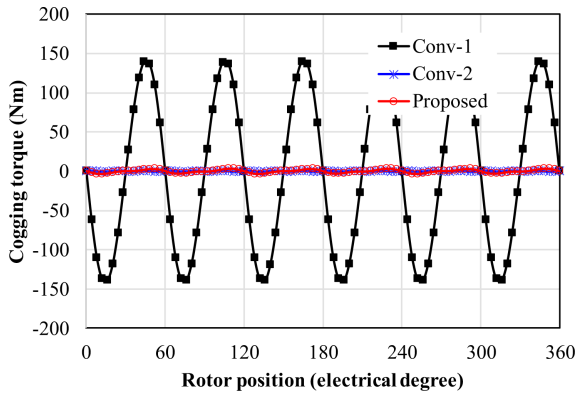

Fig. 10. (Color online) Cogging torque waveforms.

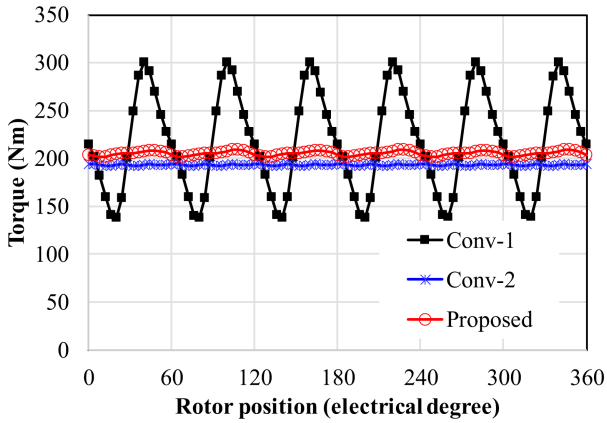

Fig. 11. (Color online) On-load torque waveforms under rated conditions.

when two winding sets are fed by their independent current. Since the rotor structure of the three electric machines is the surface PM type with negligible magnetic reluctance torque, only q-axis current control is used. From the Fig. 11, it can be seen that the average torque of the Conv-1 with conventional OL winding is slightly larger than that of the Proposed. In addition, the average torque of the Conv-2 is smaller than the Proposed because the coil span of the proposed winding was increased as shown in Fig. 5. It should be noted that only the proposed machine can adjust the coil span.

Since the three machines have different winding topologies, their corresponding inductances will exhibit different characteristics. It is necessary to observe the mutual inductances because they represent the criterion to ascertain the magnetic mutual coupling under faulty conditions. A low mutual inductance value indicates that the two winding sets are independent, implying that even if one winding set fails, the machine can still operate safely. Moreover, synchronous inductances such as the d- and q-axis inductances can indicate a capacity to withstand

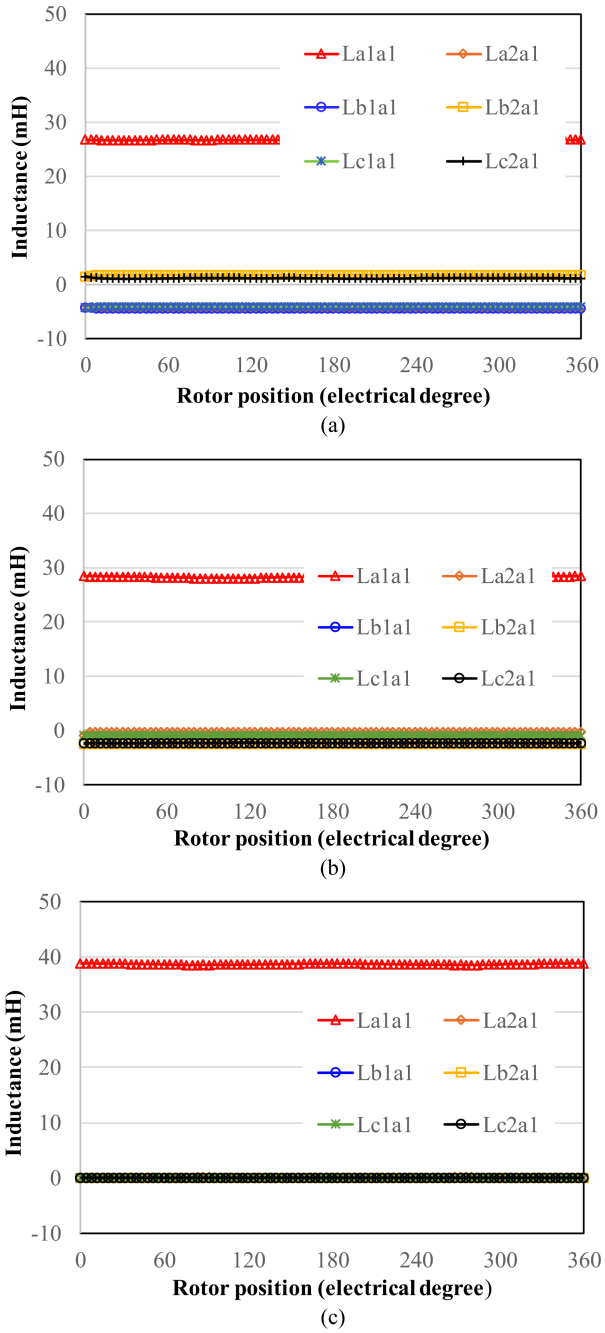

Fig. 12. (Color online) Phase inductance waveforms under rated conditions. (a) Conv-1. (b) Conv-2. (c) Proposed.

short-circuit faults. The larger synchronous inductances are better to reduce the short-circuit current [15].

Figure 12 shows the comparison results of the phase inductances. Table 2 summarizes the average values of the inductance waveforms. Mutual phase inductances are negligible in the proposed winding, whereas the ratio of mutual inductance to self-inductance in the Conv-1 is about 16 %.

From the Table 2, the values of Ldq for the three

Table 2. Inductances.

Item (mH)	Conv-1	Conv-2	Proposed
L_{A1A1} (%)	26.7 (100 %)	28.6 (100 %)	38.6 (100 %)
L_{B1A1} (%)	−4.43 (16.10 %)	−0.99 (3.47 %)	0.004 (0.01 %)
L_{C1A1} (%)	−4.43 (16.10 %)	−0.99 (3.47 %)	0.004 (0.01 %)
L_{A2A1} (%)	−4.43 (16.10 %)	−0.99 (3.47 %)	0.006 (0.01 %)
L_{B2A1} (%)	1.70 (6.33 %)	−2.50 (8.75 %)	0.006 (0.01 %)
L_{C2A1} (%)	1.10 (4.30 %)	−2.50 (8.75 %)	0.006 (0.01 %)
L_d	26.94	28.52	38.42
L_q	26.95	28.52	38.42
L_{dq}	0.00	0.00	0.00
L_{d1d2}	−5.64	1.25	0.00

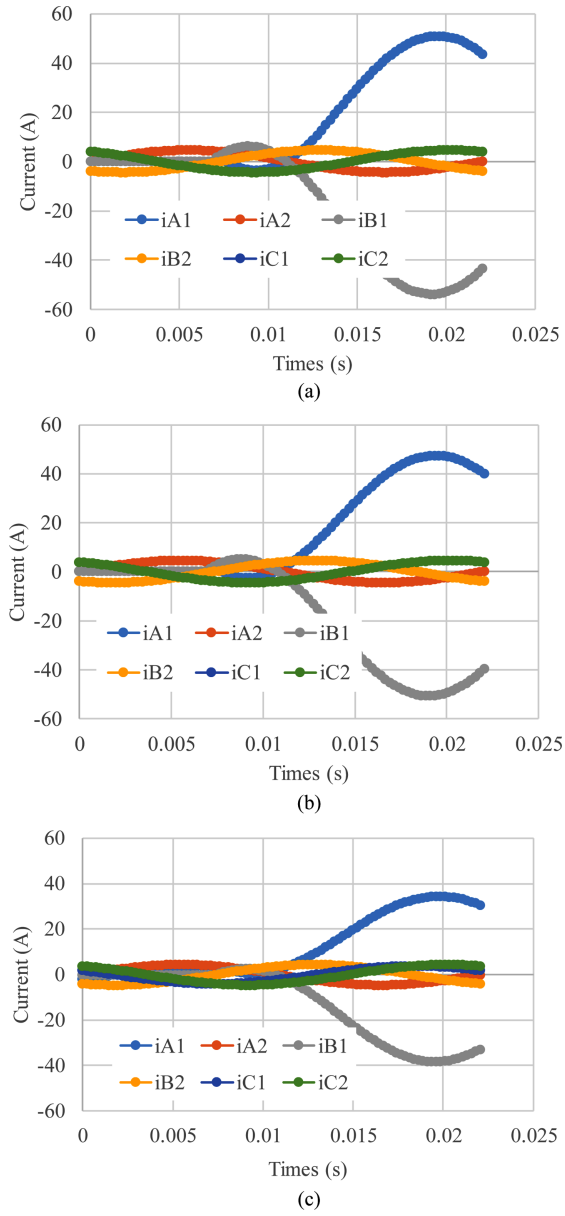

Fig. 13. (Color online) Current waveforms under short-circuit conditions. (a) Conv-1. (b) Conv-2. (c) Proposed.

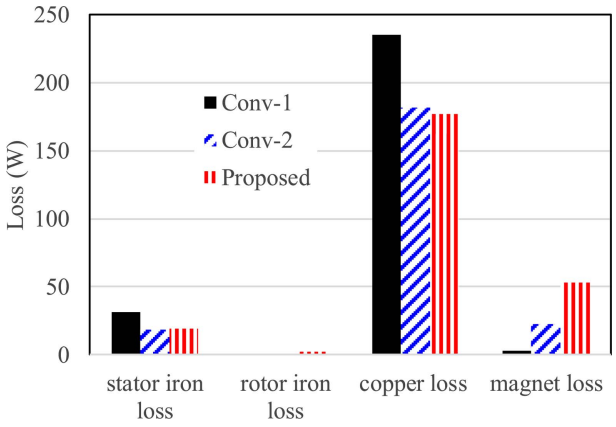

Fig. 14. (Color online) Comparsion of loss components.

machines are zero and it means that there is no magnetic cross-coupling between the d-and q-axis. The Ld and Lq synchronous inductances of the proposed machine is 42 % larger than that of Conv-1, which implies that the proposed winding topology is safer under short-circuit fault condition.

The current waveform under short-circuit condition are compared as shown in Fig. 13. It can be seen that the maximum current of the proposed winding become smallest as it has the largest inductances as presented in Fig. 12.

In order to investigate the influence of winding configuration on losses, iron loss, magnet loss, and stator copper losses have been calculated as shown in Fig. 14. The stator iron loss of Conv-1 is larger than that of the others because the more number of slot is more rotating iron loss. Since the rotor yoke is far from the air-gap, the armature reaction effect is quite small and then the rotor iron losses became negligible. In the case of Conv-1, the largest copper loss has been estimated due to the large end-winding length, whereas the magnet loss becomes the largest for the proposed winding.

The air gap flux density waveforms when only the rated stator current is excited are shown in Fig. 15(a). From the Fig. 15(b), it is confirmed that the proposed winding has both sub-harmonic components and higher harmonic component, which means that asynchronous magneto-motive force (MMF) induce eddy-current loss in permanent magnet. It is interesting that the sub-harmonic component of the proposed winding is larger than that of the Conv-2 having same poles and slots. It is well known that the harmonic contents of the MMF will incur the rotor loss [16]. Because the harmonic contents will asynchronously rotate compared with the fundamental MMF, they induce the rotor loss. In particular, the larger the harmonic amplitude or the closer the harmonic component is to the

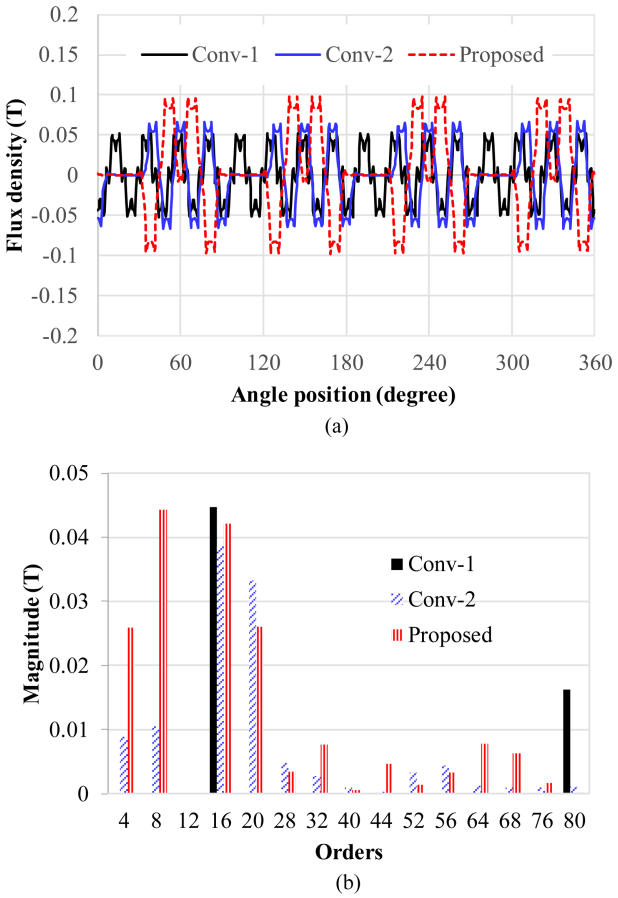

Fig. 15. (Color online) Field distribution due to armature current only. (a) Air gap flux density waveforms. (b) Harmonic orders.

fundamental, the greater the effect. Therefore, from the Fig. 15, the proposed winding induces a large magnet loss compared with the others. As pointed out in [16], it is presumed that the low-order harmonic component of the MMF in the proposed winding caused the large permanent magnet loss.

4. Conclusion

A novel winding structure for modular dual 3-phase PM machine using NOL winding has been proposed to primarily reduce the mutual inductance between phases. Three dual 3-phase machines are selected to investigate the influence of winding structure on machine performances. It has been confirmed from several simulation results that the electric machine with the proposed winding has high synchronous inductance and negligible mutual inductance, implying that the proposed winding guarantees safer operation under faulty conditions. Moreover, it has the advantage of lower torque ripple, stator iron loss, and

copper loss. However, it has larger magnet losses due to both sub- and higher harmonics MMF components. Thus, the magnet loss needs to be actively reduced by radial and axial segmentation.

Acknowledgments

This work was supported by the National Research Foundation of Korea (NRF) grant funded by the Korea government (MSIT) (No. 2017R1C1B1008128).

References

[1] J. K. Park, C. Babetto, G. Berardi, J. Hur, and N. Bianchi, IEEE Trans. Ind. **57**, 3 (2021).
[2] E. A. Klingshirn, IEEE Trans. Power App. Syst. PAS-**102**, 1 (1983).
[3] J. M. Apsley, et al. Inst. Elect. Eng.-Elect. Power Appl. **153**, 6 (2006).
[4] A. R. Munoz and T. A. Lipo, IEEE Trans. Ind. Appl. **36**, 5 (2000).
[5] R. H. Nelson and P. C. Krause, IEEE Trans. Power App. Syst., PAS-93, 3 (1974).
[6] E. F. Fuchs and L. T. Rosenberg, IEEE Trans. Power App. Syst., PAS-93, 6 (1974).
[7] L. Alberti and N. Bianchi, in Proc. 2010 ICEM, (2010).
[8] N. Bianchi and M. Dai Pre, IEE Proc. Electric Power Applications **153**, 3 (2006).
[9] N. Bianchi, et al., IEEE Trans. Ind. Appl. **42**, 4 (2006).
[10] N. Bianchi, S. Bolognani, and M. D. Pré, IEEE Trans. Ind. Appl. **44**, 5 (2008).
[11] M. Barcaro, N. Bianchi, and F. Magnussen, IEEE Trans. Ind. Appl. **46**, 6 (2010).
[12] M. Barcaro, et al., IEEE Trans. Ind. Electron. **58**, 9 (2011).
[13] M. Barcaro, N. Bianchi, and F. Magnussen, in Proc. 2009 IEMDC (2009).
[14] E. Fornasiero, et al., IEEETrans. Ind. Appl. **49**, 3 (2013).
[15] P. Xu, et al., IEEE Transactions on Industrial Electronics **65**, 3 (2018).
[16] N. Bianchi, et al., IEEE Trans. Energy Conversion **24**, 4 (2009).